

# High Performance of Chitosan-co-Polyacrylamide-TiO<sub>2</sub> Crosslinked Glutaraldehyde Hydrogel as Soil Conditioner for Soybean Plant (*Glycine max*)

Halimahtussaddiyah Ritonga<sup>1</sup>, Muhammad Ihram Basri<sup>1</sup>, Fransiskus S. Rembon<sup>2</sup>,  
La Ode Ahmad Nur Ramadhan<sup>1</sup>, Muhammad Nurdin<sup>1\*</sup>

<sup>1</sup>Department of Chemistry, Faculty of Mathematics and Natural Sciences, Universitas Halu Oleo, Kendari 93232, Southeast Sulawesi, Indonesia

<sup>2</sup>Department of Soil Science, Faculty of Agriculture, Universitas Halu Oleo, Kendari 93232, Southeast Sulawesi, Indonesia

\* Prof. Muhammad Nurdin, Ph.D, mnurdin06@yahoo.com, ORCID ID: <https://orcid.org/0000-0002-6727-9283>

## Abstract

Received: 10.01.2020  
Accepted: 29.07.2020  
Associated editor: J. Antonkiewicz

## Keywords

Composite  
Hydrogel  
Soil conditioner  
Swelling  
TiO<sub>2</sub>

Research on hydrogels as soil conditioners has been developed based on hydrogels copolymerized with composite materials in the form of chitosan and TiO<sub>2</sub> to overcome low physical properties and low swelling of polyacrylamide. The aims of the study are synthesis, characterization, application of hydrogels, and determination of the physical and chemical properties of soil and the growth of soybean plants. Synthesis of chitosan-co-polyacrylamide-TiO<sub>2</sub> crosslinked glutaraldehyde hydrogel was prepared by the chemical crosslinking method. The characterization of hydrogel was performed by using Fourier Transform Infra-Red (FTIR) and Scanning Electron Microscope (SEM). FTIR spectrum shows the functional groups of chitosan co-polyacrylamide-TiO<sub>2</sub> crosslinked glutaraldehyde which includes OH functional groups (3408.22 cm<sup>-1</sup>), NH (1602.85 cm<sup>-1</sup>), C=O (1502 cm<sup>-1</sup>), CN (1600.92 cm<sup>-1</sup>), and Ti-O (619.15 cm<sup>-1</sup>). The SEM image shows the formation of pores and cavities in the hydrogel. The application of hydrogels in soybean plants shows differences in physical and chemical properties of soil and plant growth. The use of all variations of hydrogel had no significant effect on soil physical properties including temperature, humidity, and bulk density. Meanwhile, hydrogels with TiO<sub>2</sub> concentration of 60 ppm influence significantly to the chemical properties of soil such as organic carbon, cation exchange capacity (CEC), and level of nitrogen, phosphorus, and potassium in the soil. The optimum number of leaves, plant height, total dry weight are 68 leave blades, 207 cm, and 20.6 g, respectively. This optimum condition was found in the use of KTiKPAG60 hydrogel. The results showed that chitosan-co-polyacrylamide-TiO<sub>2</sub> crosslinked glutaraldehyde has the potential to be a soil conditioner.

## 1. Introduction

The utilization of natural hydrogels in agriculture has been developed by various hydrogel ingredients and synthesized for utilizing as soil conditioners. Soil conditioner is important to solve the problem of dry land because of its ability to storing groundwater. In addition, the use of hydrogels in agriculture is also used to reduce the tendency of soil compaction, prevent erosion, and improve the efficiency of fertilizer used (Rajakumar and Sankar, 2016).

Natural or synthetic material hydrogels have been widely used such as polyacrylamide (PAAM) with acrylamide monomers. However, polyacrylamide polymers have several disadvantages such as their limitation of water absorption ability and is a homopolymer with relatively low physical properties cause

the limitation of application development (Zhao et al., 2015). To improve the swelling properties and physical properties, polyacrylamide polymers is needed to modified through copolymerization process with chitosan. Meanwhile, chitosan is a polysaccharide that has bioactive properties, non-toxic, biocompatible, biodegradable, and easily modified to its derivative material (Yu et al., 2017).

Chitosan is a natural polymer derived from deacetylation of chitin composition that can be obtained from marine animals such as crab and shrimp shells. Chitosan is widely applied in various things such as cosmetic ingredients (Synowiecki and Al-Khateeb, 2003), antibacterial ingredients (Dutta et al., 2012), metal adsorption (Al-Karawi et al., 2011), food packaging (Gomes et al., 2017) and in agriculture as a soil conditioner (Abdel-Aziz et al., 2016). The role of chitosan in increasing agri-

cultural yields has been shown to increase the growth of roots, leaves, and branches in some plants such as tomatoes, cucumbers, and carrots. Chitosan can play a role in increasing plant productivity both compilation is fully applied and when used as nitrogen, phosphorus, potassium fertilizer coatings (Abdel-Aziz et al., 2016). In addition, chitosan also has the ability as an antimicrobial so it can protect plants from biotic stresses (Dutta et al., 2012). Meanwhile, chitosan has a disadvantage in its lower mechanics. It needs to add other materials to increase its mechanical strength by adding composite materials (Park et al., 2002). One inorganic material that can be used to increase mechanical strength titanium dioxide (TiO<sub>2</sub>) semiconductor.

The application of TiO<sub>2</sub> so far includes raw materials for the paint and plastic industries (Nayl et al., 2009), sensors (Nurdin et al., 2018a), environmental cleaners with their ability to degrade organic pollutants (Nurdin et al., 2016; Maulidiyah et al., 2017; Nurdin et al., 2018b) and as fertilizer biological for plants (Khater, 2015). Several studies on the use of anatase TiO<sub>2</sub> nanoparticles to improve growth, yield, and ingredients chemicals in plants have been carried out. TiO<sub>2</sub> has been shown to improve plant growth by increasing nitrogen metabolism which can further increase nitrate absorption. TiO<sub>2</sub> also accelerates the conversion of inorganic nitrogen to organic nitrogen which ultimately increases the wet weight and dry weight of plants.

TiO<sub>2</sub> compounds are also able to increase photosynthetic efficiency in plants (Khater, 2015; Giorgetti et al., 2019). With the advantages possessed by chitosan and TiO<sub>2</sub> in enhancing plant growth, in this study the binding of chitosan-TiO<sub>2</sub> was carried out to become a chitosan-TiO<sub>2</sub> composite material. The chitosan-TiO<sub>2</sub> composite will then be copolymerized with polyacrylamide into chitosan-co-polyacrylamide-TiO<sub>2</sub> composite hydrogel through the crosslinking method. Crosslinker agents that can be used can be derived from aldehydes (Maitra and Shukla, 2014), urea derivatives, and carboxylic acids (Ciolacu et al., 2012). Glutaraldehyde is a cross-linker that is widely applied in the preparation of hydrogels. The amine group from -NH<sub>2</sub> found in chitosan-co-polyacrylamide-TiO<sub>2</sub> will attack the carbonyl group, C=O in glutaraldehyde which will produce a new bond C=N. So far, the use of TiO<sub>2</sub> in agriculture has been applied in the form of foliar spray and direct addition of TiO<sub>2</sub> nanoparticles into the soil with variations in concentrations of 10, 20, 30, 40, 60, and 80 ppm for *Triticumaestivum* L (Rafique et al., 2018).

However, the study on the addition of TiO<sub>2</sub> in hydrogel composite for slow and simultaneous controlled releasing of fertilizer and other nutrients in the soil for soybean plant is not conducted yet. Therefore, research on the application of chitosan-co-polyacrylamide-TiO<sub>2</sub> crosslinked glutaraldehyde hydrogel as a soil conditioner for soybean plants was conducted. During the growth period until the harvest period is analyzed the physical-chemical properties of soil include pH, temperature, CEC (cation exchange capacity), organic carbon, bulk density of soil, and absorbed levels of nitrogen, phosphorus, potassium fertilizer. Meanwhile, in terms of soybean growth, it was observed plant height, total leaves, and total dry weight of soybean plants.

## 2. Materials and methods

### 2.1. Material

Chitosan used in this study was prepared by the deacetylation method of chitin derived from shrimp shells (*Penaeus Monodon*) with the method according to Sewvandi and Adikary (2012) with degree of deacetylation and molecular weight chitosan (Mv) 83.8% and  $2.27 \times 10^5$  Dalton, respectively. TiO<sub>2</sub> powder was prepared by sol gel method with controlled hydrolysis of titanium (IV) isopropoxide (TTIP) (Weldermarian and Welderfael, 2015). The materials for making hydrogels include acrylamide, benzoyl peroxide, acetic acid 2%, and glutaraldehyde as cross linkers.

### 2.2. Synthesis of hydrogel chitosan-co-polyacrylamide-TiO<sub>2</sub> crosslinked glutaraldehyde

Synthesis of hydrogel chitosan-co-polyacrylamide-TiO<sub>2</sub> crosslinked glutaraldehyde by chemical method using benzoyl peroxide as an initiator (Ritonga et al., 2019) with the addition of variations in the concentration of TiO<sub>2</sub> 10, 20, 30, 40, 60, and 80 ppm in hydrogel suspension. The characterization of hydrogels was carried out by FTIR and SEM and the synthesis of hydrogel swelling results according to Formula 1.

### 2.3. Swelling test

To determine percentage of swelling, Hydrogel (g) was immersed in 100 mL of distilled water. The mixture is then filtered using filter paper for 10 minutes. The amount of absorbed water is calculated as Formula 1 follows:

$$\% \text{Swelling} = \frac{G_s - G_i}{G_i} \times 100\% \quad (1)$$

Where G<sub>s</sub> is the weight swelling of the hydrogel and G<sub>i</sub> is the initial weight of the polymer sample (Zhou et al., 1996).

### 2.4. Application of hydrogel

For application of hydrogel, Argomulyo varieties of soybean plants were obtained from the Seed Hall in Kendari City, South-east Sulawesi, Indonesia. Planting is carried out in greenhouses, from the end of January to April 2019 when the summer ends and the entry of the rainy season. It is conducted in polybags (40 cm × 40 cm) with weight of soil per polybag approximately ±10 kg. Hydrogel 10 g was added to each polybag. Plant maintenance is carried out by watering 100 mL of water, meanwhile observations are carried out every 5 days.

### 2.5. Analysis of the physical, chemical properties of soil

Soil pH test was determined by the method of Ritonga et al. (2019). Determination of soil organic carbon content was determined by the method of Pivato et al. (2016). Determination of land CEC was determined by the method of the Agricultural Research and Development Agency of the Ministry of Agricul-

ture Ritonga et al. (2019). Determination of soil bulk density was determined by the method of Pivato et al. (2016).

## 2.6. Analysis of Soybean Plant Growth

Analysis of leaf number and plant height was determined manually. Analysis of plant dry weight was determined by Wood and Roper (2000).

## 2.7. Data Analysis Techniques

Measurement results of physical properties of soil (temperature, humidity, bulk density), chemical properties of soil (pH, C-organic, CEC, nitrogen, phosphorus, potassium), total nitrogen levels (Kjeldahl method with  $H_2SO_4$  ashing and absorbance measurements using UV-Vis spectrophotometer  $\lambda = 636$  nm), total phosphorus and total potassium soil were prepared using 25% HCl extractor and measurement of total phosphorus absorbance using UV-Vis spectrophotometer  $\lambda = 710$  nm while total phosphorus and potassium were prepared using 25% HCl extractor and measurement of total phosphorus absorbance using UV-Vis spectrophotometer  $\lambda = 710$  nm while potassium total using atomic absorption spectroscopy method. Plant measurement data (total dry weight, plant height, number of leaves) (before and after harvest) analyzed descriptively and inferentially.

Descriptive analysis aims to describe the average value and standard deviation of the physical chemical properties and growth of soybean plants after planting. Inferential analysis examines the effect of treatment (administration of hydrogels) on changes in physical and chemical properties of soil and their effects on plant growth. Inferential analysis using the analysis of variance (ANOVA) method and the Duncan test method. All analyzes, both description and inferential, were carried out using SPSS version 22 software.

## 3. Results and discussion

### 3.1. Synthesis of hydrogel chitosan-co-polyacrylamide-TiO<sub>2</sub> crosslinked glutaraldehyde

Hydrogel synthesis carried out in this study was carried out by crosslinking copolymerization technique. Chitosan first interacts with the initiator of benzoyl peroxide before interacting with a mixture of acrylamide and glutaraldehyde monomers as crosslinkers. During the synthesis process, nitrogen gas has flowed which functions to remove oxygen in the system when synthesizing. This is done because oxygen can inhibit the formation of copolymers through peroxide formation and vice versa encourage the formation of homopolymers (Ritonga et al., 2019). In addition, the temperature factor also affects the speed of combining the polyacrylamide chain.

Stages of polymerization reactions consist of initiation, propagation, and termination reactions. The phase of the polymerization reaction begins with the initiation process by benzoyl peroxide radical initiator. At a temperature of 60–70°C benzoyl peroxide undergoes homolytic breaking of bonds and produces benzyloxy free radicals. Benzyloxy radicals will contain double bonds in the monomers, resulting in polyacrylamide monomer radicals being formed. The proposed reaction stage of initiation can be seen in Fig 1. At the propagation stage, the copolymerization reaction occurs between chitosan and acrylamide where the radical chain formed at the initiation stage will increase the length of the polymer chain. The propagation reaction stops when the monomer has reacted in Fig. 2. The termination stage is the final stage of the polymerization reaction. At the termination stage, two radical polymers will join or transfer of hydrogen from one end to the other (disproportionation). Termination occurs by means of a combination of combining the radical structure of the end of the chain to produce grafted chitosan-co-polyacrylamide (Fig. 3).

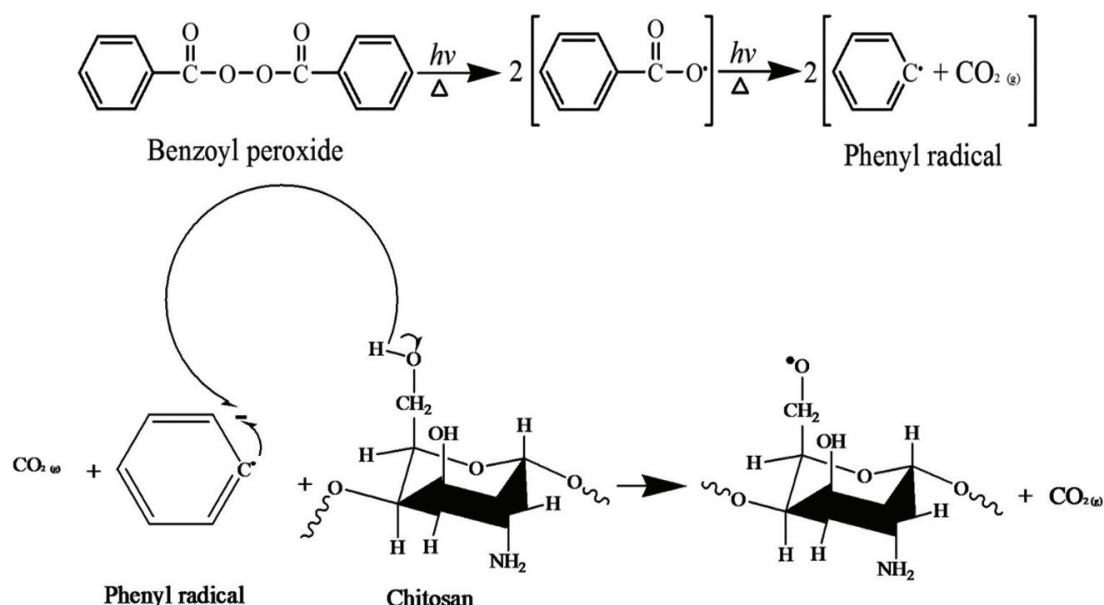


Fig. 1. Proposed reaction phase initiation mechanism

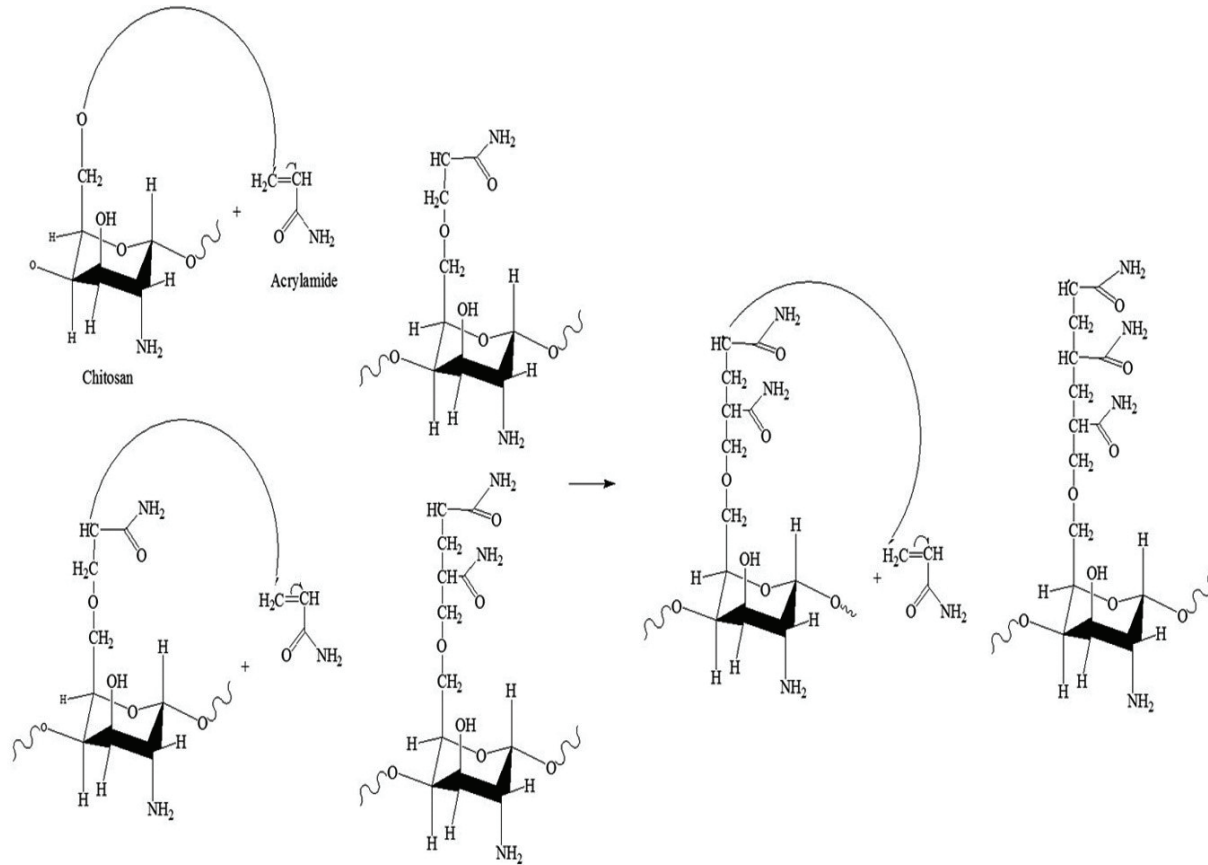


Fig. 2. Proposed chitosan copolymerization mechanism

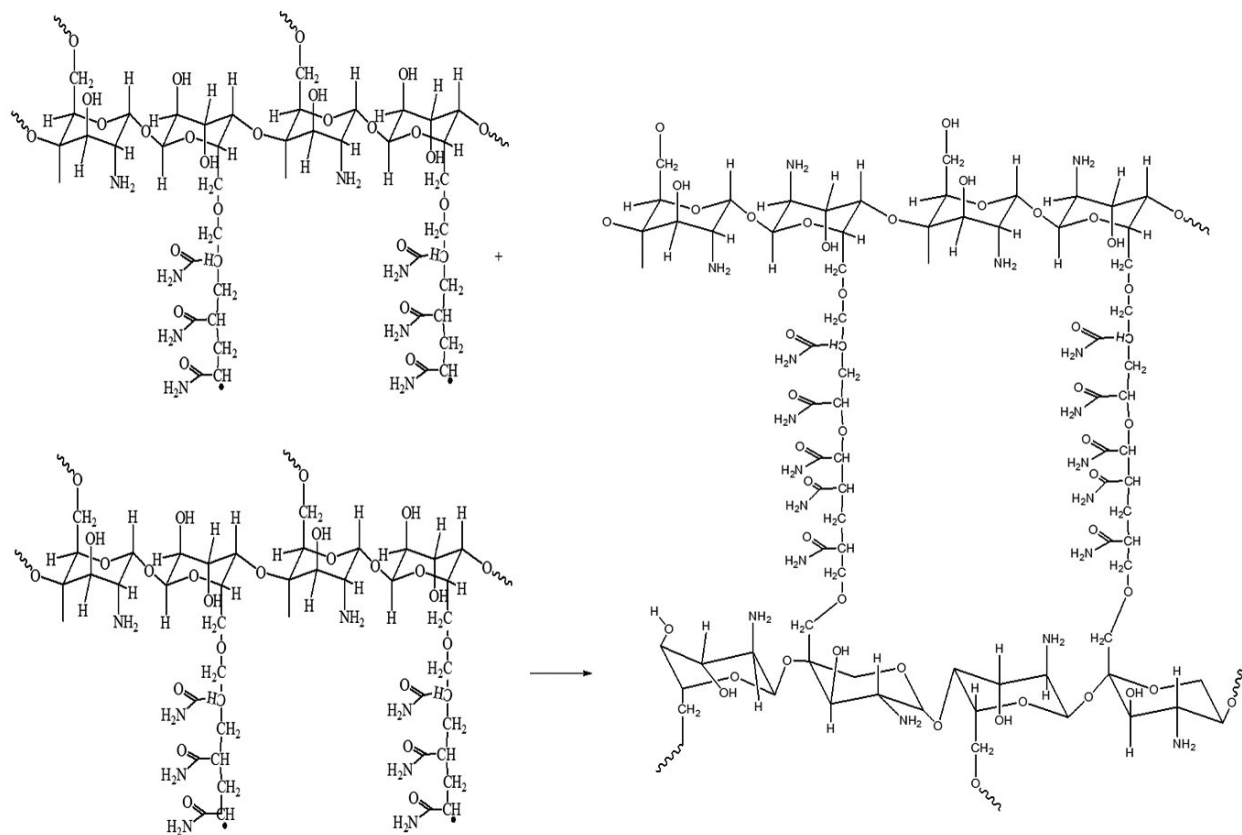


Fig. 3. Proposed mechanism of termination of chitosan-co-polyacrylamide

Furthermore, the suspension of chitosan-co-polyacrylamide was added by  $\text{TiO}_2$  by reflux for 1 hour at a temperature of  $60\text{--}70^\circ\text{C}$  and crosslinking of glutaraldehyde was added to form a hydrogel chitosan-co-polyacrylamide- $\text{TiO}_2$  bound to glutaraldehyde. The aldehyde group in glutaraldehyde will bind to the amine group in chitosan that forms covalent bonds that will connect one chitosan polymer to another. The addition of glutaraldehyde as a crosslinking agent can affect the physical properties of the hydrogel produced.  $\text{TiO}_2$  enters at the end of the chitosan chain in accordance with the proposed reaction from Pathania et al. (2016). The proposed structure of chitosan-co-polyacrylamide- $\text{TiO}_2$  crosslinked glutaraldehyde can be seen in Fig. 4.

Fig. 4 is a proposed crosslinking mechanism of chitosan-co-polyacrylamide- $\text{TiO}_2$  crosslinked glutaraldehyde. The reaction showed that the  $\text{--OH}$  group of chitosan interacted with Ti from the surface of  $\text{TiO}_2$ .  $\text{TiO}_2$  also experiences interaction with the surface of chitosan, because the presence of amino groups in chitosan can interact with Lewis  $\text{TiO}_2$  acid (El Kadib and Bousmina, 2012).  $\text{TiO}_2$

which has bonded with chitosan will react with other  $\text{TiO}_2$  which is soluble in water. Based on this reaction, it can be seen that new bonds have been formed in the form of  $\text{C=N}$  and  $\text{Ti-O}$  bonds.

### 3.2. Characterization of hydrogel Chitosan-co-Polyacrylamide- $\text{TiO}_2$ crosslinked glutaraldehyde

#### 3.2.1. Analysis fungsional group using the Fourier Transform Infrared (FTIR)

Functional group analysis is one way to find out the chemical characteristics and success of the synthesis that has been carried out based on chitosan functional groups into hydrogel chitosan-co-polyacrylamide- $\text{TiO}_2$  crosslinked glutaraldehyde using the Fourier Transform Infrared (FTIR) instrument. The infrared spectrums show any functional groups contained in a compound based on wave numbers and transmittance. FTIR spectrums analysis of hydrogel chitosan-co-polyacrylamide- $\text{TiO}_2$  crosslinked glutaraldehyde are shown in Fig. 5.

Fig. 4. Proposed interaction of chitosan co-polyacrylamid  $\text{TiO}_2$  with glutaraldehyde

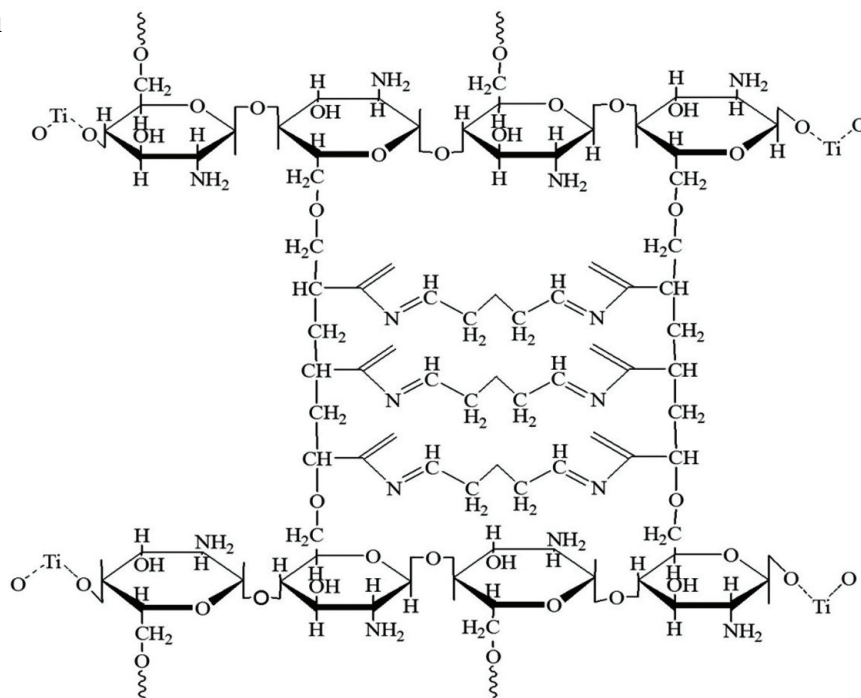
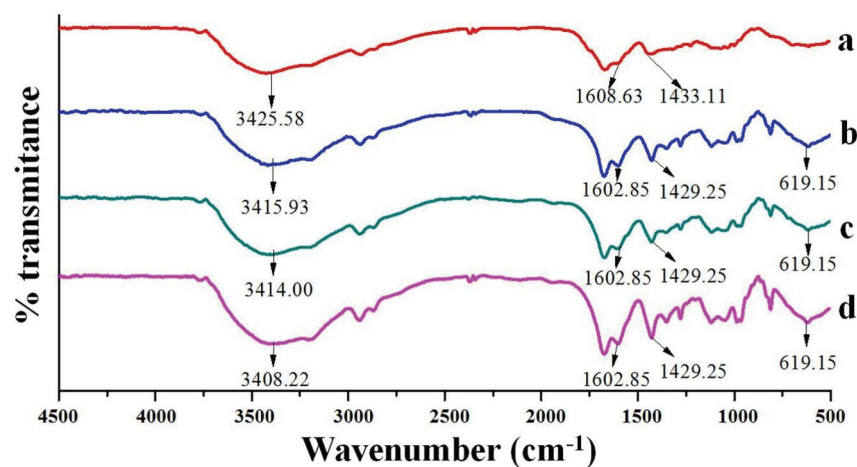


Fig. 5. FTIR spectrum (a) KKPAG (b) KTiKPAG40 (c) KTiKPAG60 (d) KTiKPAG80



Based on Fig. 5 the results of the infrared spectrum of hydrogels crosslinked glutaraldehyde with variations in  $\text{TiO}_2$  concentrations indicate specific changes that occur after the addition of  $\text{TiO}_2$  and glutaraldehyde, exhibited in wavenumbers  $1500\text{--}1700\text{ cm}^{-1}$  which is the absorption peak of C=N group of hydrogels crosslinked glutaraldehyde. This identified the carbonyl group (C=O) of glutaraldehyde to react with  $\text{NH}_2$  from polyacrylamide. Based on the spectra obtained by absorption peaks at wavenumber  $1400\text{--}1600\text{ cm}^{-1}$  showed specific absorption of C=N bonds which indicated that hydrogel chitosan-co-polyacrylamide- $\text{TiO}_2$  crosslinked glutaraldehyde was successfully synthesized. Whereas according to Haidar et al. (2015) state that the Ti-O group was identified between wavenumbers  $400\text{--}700\text{ cm}^{-1}$ . This was shown at the absorption peak of wavenumber  $619.15\text{ cm}^{-1}$  contained in the FTIR results of hydrogel chitosan-co-polyacrylamide- $\text{TiO}_2$  bound to glutaraldehyde. Based on the results of the interpretation obtained from the FTIR spectrum, it showed that the hydrogen chitosan-co-polyacrylamide- $\text{TiO}_2$  crosslinked glutaraldehyde has been successfully synthesized.

### 3.2.2. Morphological analysis using Scanning Electron Microscope (SEM)

Morphological characterization of hydrogels was carried out using a Scanning Electron Microscope (SEM) to determine the surface morphology of hydrogel chitosan-co-polyacrylamide- $\text{TiO}_2$  crosslinked glutaraldehyde samples which were successfully synthesized with 2500x magnification. Hydrogels that have many cavities can allow more water absorption than other hydrogels. Gao et al. (2008) state that absorption capacity is influenced by two factors, namely bulk density and number of cavities. The more the number of cavities the greater the absorption capacity and the greater the bulk density the smaller the absorption capacity.

Fig. 6 (a) shows that on the surface of the hydrogel chitosan-co-polyacrylamide- $\text{TiO}_2$  crosslinked glutaraldehyde has a number of pores clearly visible on the surface of the hydrogel compared to Fig. 6 (b). Fig. 6b shows the SEM results of hydrogel

chitosan-co-polyacrylamide- $\text{TiO}_2$  crosslinked glutaraldehyde, along with increasing  $\text{TiO}_2$  concentrations, the pores on the surface of the hydrogel are seen to be covered and cavities form. In hydrogel chitosan-co-polyacrylamide- $\text{TiO}_2$  crosslinked glutaraldehyde with a concentration of 60 ppm (e)  $\text{TiO}_2$  showed that the cavities on the surface of the hydrogel were increasing when compared with Fig. 6(d). While in Fig. 6(f) which is the morphology of hydrogel chitosan-co-polyacrylamide- $\text{TiO}_2$  crosslinked glutaraldehyde with a concentration of  $\text{TiO}_2$  of 80 ppm it has a smooth surface shape and tends to have fewer cavities. This indicates that variations in the concentration of different  $\text{TiO}_2$  result in a different surface structure.

### 3.2.3. Swelling test of hydrogel chitosan-co-polyacrylamide- $\text{TiO}_2$ crosslinked glutaraldehyde

Degree of swelling is the ability of a material to expand larger than the initial weight. The swelling ratio is the ratio of the hydrogel weight ratio in the state of absorbing water (swelling) to its dry weight. Elliott (2004) suggested that superabsorbent polymers when putting into water or solvents would experience swelling resulting in interactions between polymers and water molecules. Water will be diffused by superabsorbent polymers because of the presence of hydrophilic groups namely  $\text{NH}_2$  groups on chitosan and OH groups. After reaching the equilibrium stage, absorbed water will be bound to the carboxylic group(-COOH) to form hydrogen bonds. In the end, the absorbed water will remain suspended in the superabsorbent polymer so that the polymer undergoes swelling (Bian et al., 2018).

The hydrogel is a hydrophilic framework that is cross-linked and has the capacity to swell by absorbing water but is insoluble due to crosslinking. The swelling ratio property was conducted to determine the ability to expand from a hydrogel to water absorb. The character of the swelling hydrogel is also influenced by the chemical structure of the polymer making up the hydrogel. Hydrogel chitosan-co-polyacrylamide- $\text{TiO}_2$  crosslinked glutaraldehyde experienced swelling on each variation of  $\text{TiO}_2$  concentration as showed Table 1.

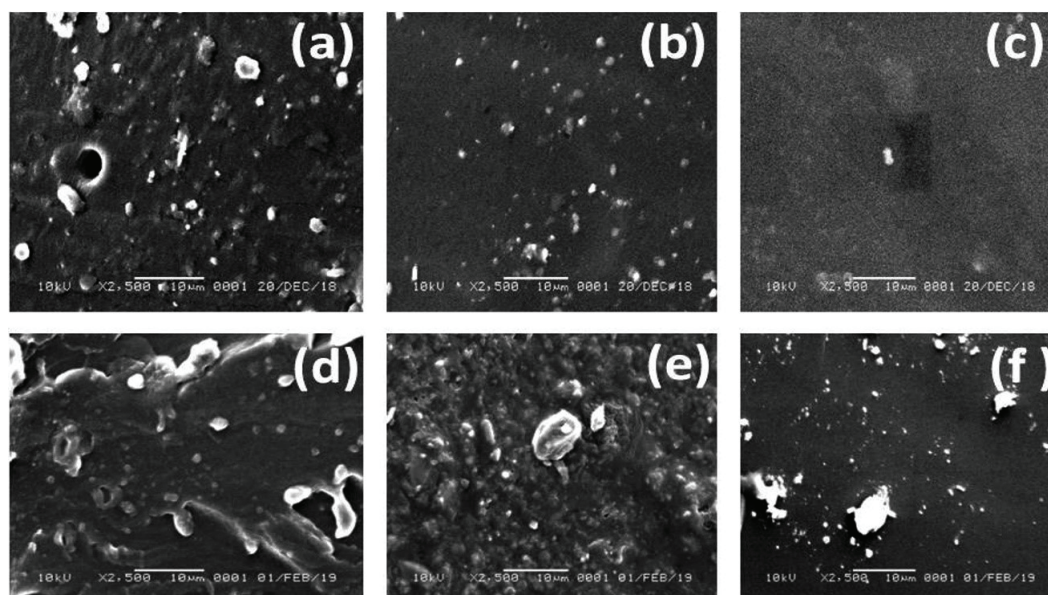


Fig. 6. (a) Hydrogel chitosan-co-polyacrylamide- $\text{TiO}_2$  crosslinked glutaraldehyde with variations in  $\text{TiO}_2$  concentration of 10 ppm, (b) 20 ppm, (c) 30 ppm, (d) 40 ppm, (e) 60 ppm (f) 80 ppm at 2500x magnification

**Table 1**  
The ratio of swelling to the composition of the hydrogel

Sample code	Weight before soaking (g)	Weight after soaking (g)	Swelling (%)
KKPAG	3.02	14.03	364.76
KTiKPAG10	3.00	5.69	89.67
KTiKPAG20	3.05	5.54	81.64
KTiKPAG30	3.03	5.56	83.50
KTiKPAG40	3.04	5.70	87.50
KTiKPAG60	3.05	6.10	100.00
KTiKPAG80	3.04	5.06	66.45

From Table 1, showed a tendency to swelling different variations of TiO<sub>2</sub> concentrations. The hydrogels without TiO<sub>2</sub> show the greatest swelling results (364.76%) when compared to hydrogels containing TiO<sub>2</sub>, the swelling of hydrogels with TiO<sub>2</sub> were 89.4%, 89.67%, 81.64%, 83.5%, 87.5%, 100%, and 66.45%, respectively. This is due to the hydrophilic group on the hydrogel containing TiO<sub>2</sub> such as OH and NH<sub>2</sub> groups have interacted with the TiO<sub>2</sub> structure, thus blocking the diffusion of water in the hydrogel polymer network.

**3.2.4. Analysis of the properties of soil physics**

Analysis of physical properties and chemical properties of soil greatly affects plant performance in growth. Soil chemistry includes analysis of organic carbon, nitrogen, phosphorus, po-

tassium, and CEC levels. Physical properties of soil include temperature, humidity, pH, bulk density. The soil temperature in soybean plants influences the growth of Rhizobium, roots, and soybean plants, especially closely related to the germination process, height addition and stem segments, flowering, nutrient uptake, and filling of pods. The interaction between the temperature-intensity of sunlight-soil moisture greatly affects the rate of growth of soybean plants. The effect of adding hydrogels to soil temperature and the effect of hydrogels on time (days) can be seen in Fig. 7a and 7b.

Based on temperature observations on all polybags, there were no significant differences in each measurement. The temperature that is suitable for the growth of soybean plants ranges from 22–27°C while based on the results of the measurement of

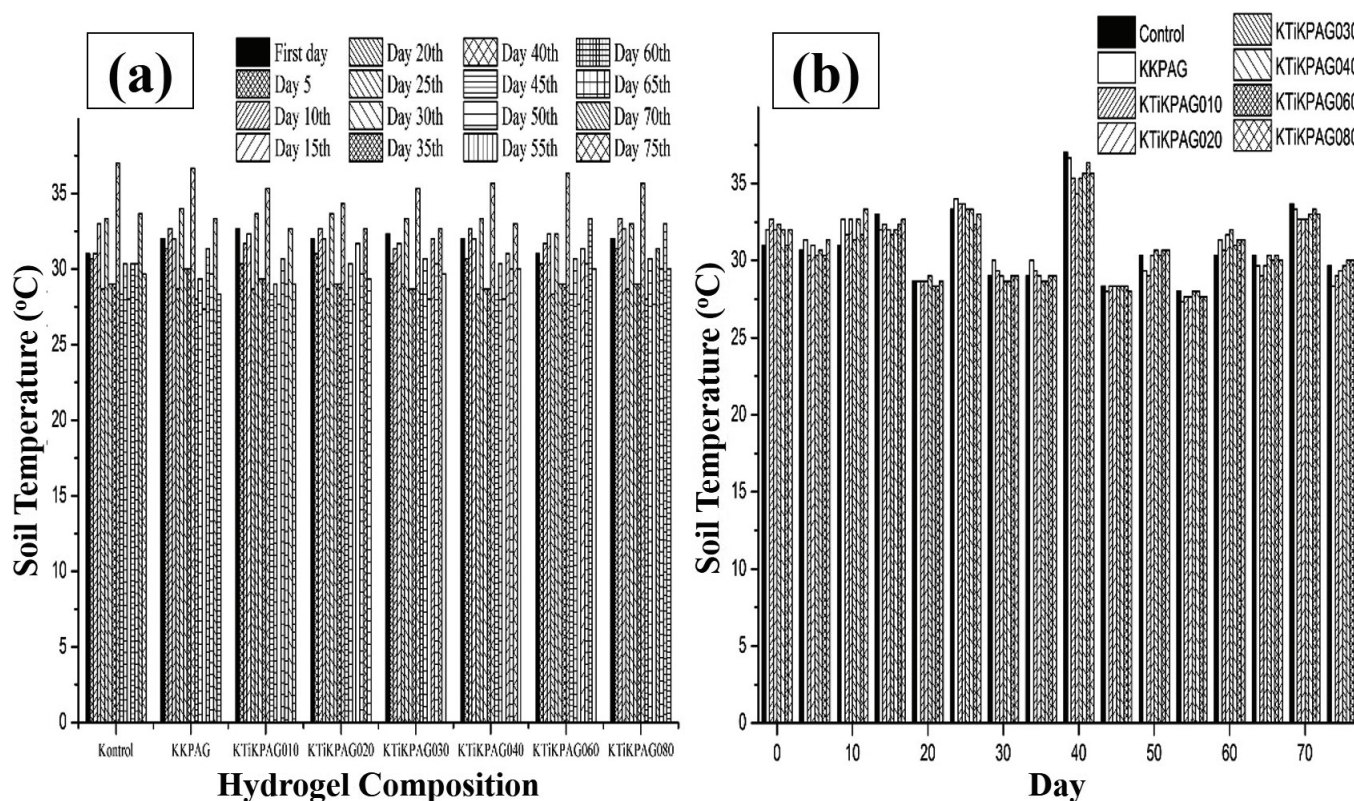


Fig. 7. Effect of (a) hydrogel composition on soil temperature, (b) Effect of soil temperature on time (days)

soil temperature ranges from 28–37°C. The highest temperature was observed in the 40<sup>th</sup>-day measurement. This happened because of the uncertainty in the weather conditions at the time of observation due to the changing seasons. The soil temperature from the analysis was quite different compared to the temperature suitable for soybean plants but still showed good performance during growth due to the adequacy of water from hydrogels added to the soil.

Soil moisture is the content of the amount of water in the soil in the area of plant roots. Low humidity will limit the metabolic process and reduce the rate of photosynthesis which results in the inhibition of fruit formation (Munyiri et al., 2010). Analysis of the effect of composition on moisture and moisture on time (days) in Fig. 8a and 8b.

Based on the measurements made, the plants in all polybags have different but not significant humidity levels at each measurement. this can be seen in Fig. 8a and 8b. In the measurement of the 10th day to the 50th day, the highest moisture level is seen in the composition of the KKPAG. This happens because the composition has a high swelling rate (Table 1).

When pH is close to neutral, the transfer of cations will be easier, so nutrients are available for plant growth (Rusan et al., 2007). In general, nutrients will be easily absorbed by plants at pH 6.6–7.5, because at that pH most nutrients will dissolve easily in water (Motsara and Roy, 2008). Result Analysis of the hydrogel composition effect on pH and the effect of pH on time (days) can be seen in Fig 9a and 9b.

Based on the measurements of soil pH carried out, the addition of hydrogels to polybags affected the soil pH but, not signifi-

cantly in all polybags on the 5th to 75th day of measurement, the pH was in the range of 7, which indicates that the use of hydrogels on the soil at each the treatment does not have a significant effect on plants using hydrogels or plants without hydrogel use hydrogels.

Based on bulk density analysis shows a significant level of difference in each administration of hydrogel, when compared to control plants. However, the increase in each treatment giving hydrogel containing TiO<sub>2</sub> is not too significantly different from each other. Soil samples for bulk density analysis are taken when the harvest period has finished and it is believed that hydrogel in the soil has been degraded so that the ability to swell hydrogel can no longer affect soil bulk density. Bulk density is theoretically influenced, among others, by soil texture, soil structure, and soil organic matter. These three factors are indirectly influenced by soil water content. In terms of soil texture, soil that is used as a fine-textured growing medium with a bulk density ranges from 0.91 to 1.18 g cm<sup>-3</sup>, whereas organic soils generally have bulk density between 1.1–6 g cm<sup>-3</sup> (Rusdi et al., 2015).

Based on bulk density analysis did not show a level of difference from each others composition but we can state that soil used in this research is a fined texture soil that has a large surface and contains many pores. This condition cause water and air circulate well in the soil.

3.2.5. Analysis of the Chemical Properties of Soil

Statistical analysis of soil chemical properties including analysis of organic carbon, nitrogen, phosphorus, potassium, and soil CEC levels. Organic carbon is an indicator to determine

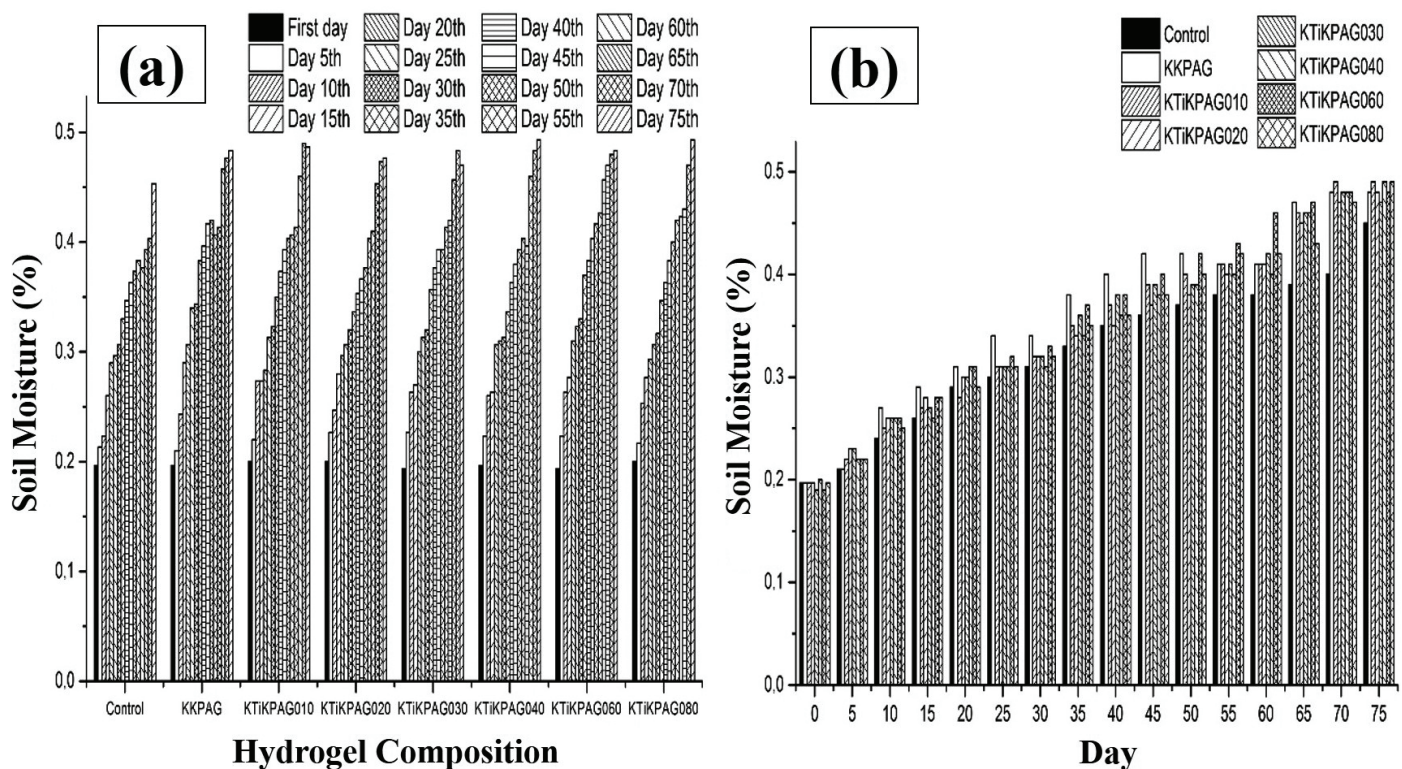


Fig. 8. Effect of (a) hydrogel composition on soil moisture, (b) soil moisture on time (days)



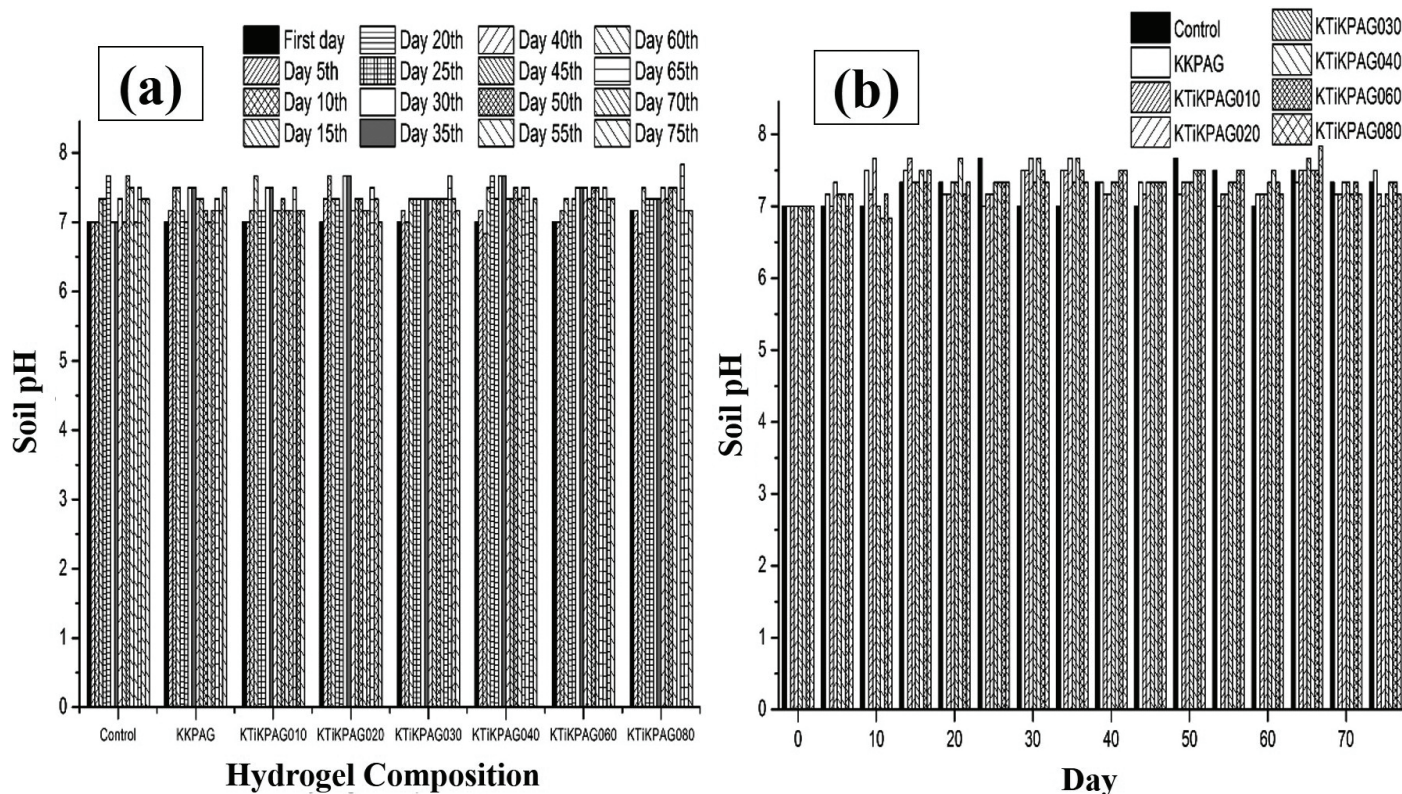


Fig. 9. Effect of (a) hydrogel composition on soil pH, (b) soil pH on time (days)

**Table 2**  
Effect of composition of hydrogels on bulk density

Treatment	Bulk Density g/cm <sup>3</sup>
Control	1.1433 a
KKPAG	1.1067 a
KTiKPAG10	1.1733 a
KTiKPAG20	1.0533 a
KTiKPAG30	1.1067 a
KTiKPAG40	1.0233 a
KTiKPAG60	1.0833 a
KTiKPAG80	1.1433 a

**Table 3**  
Statistical analysis of chemical properties of soil

Treatment	C-organic (%)	CEC (meq 100 g <sup>-1</sup> )	Total Nitrogen (%)	Total Phosphorus (ppm)	Total Potassium (ppm)
Control	2.4 a	19.0 a	0.17 a	23.6 a	10.9 a
KKPAG	2.9 ab	21.1 b	0.18 a	24.4 a	11.3 a
KTiKPAG10	3.3 ab	23.1 c	0.19 ab	24.8 a	12.1 ab
KTiKPAG20	4.1 bc	24.7 d	0.20 ab	27.0 ab	13.1 ab
KTiKPAG30	4.7 cd	24.3 cd	0.22 abc	27.3 ab	13.6 ab
KTiKPAG40	5.6 de	24.8 d	0.23 bc	28.1 ab	16.3 ab
KTiKPAG60	6.2 e	26.2 e	0.25 c	32.3 b	17.7 b
KTiKPAG80	5.1 cde	24.2 cd	0.23 bc	28.5ac	13.9 ab

The mean values followed by unequal letters in the same column differed significantly at 0.05 which was tested by the Duncan method.

the content of organic matter contained in the soil. The content of soil organic matter in the form of organic carbon must be maintained so as not less than 2%. According to Griffin et al. (2003), the content of normal organic carbon according to soil nutrient criteria is 2.1–3.0%. Statistical analysis of organic carbon levels can be seen in Table 3.

Based on the statistical analysis the difference in organic carbon between plants without hydrogels is quite different significantly from the whole plant given the addition of hydrogels, especially in the composition of KTiKPAG60 which tends to have

very high organic carbon content and is significantly different from control plants, KKPAG, KTiKPAG10, KTiKPAG20, and KTiKPAG30.

Cation exchange capacity (CEC) is a chemical property that is closely related to soil fertility (Rashidi and Seilsepour, 2008). The higher the CEC, the higher the fertility of the soil due to the level of organic carbon is also higher so that the potential productivity of the plant increases as well as vice versa. Statistical analysis of cation exchange capacity can be seen in Table 3.

Based on the statistical analysis, differences in soil CEC between plants without hydrogels were quite significantly different from the overall plants given the addition of hydrogels, especially in the composition of KTiKPAG60 which tended to have a very high CEC compared to other compositions.

Nutrients of nitrogen, phosphorus, and potassium are macronutrients that are needed for plant growth. Nitrogen is the main limiting factor because it is often deficient because it is easily soluble, easily washed, and evaporates. This element is also a constituent of plant proteins, chlorophyll, and nucleic acids so that it can spur the production of green plants and can increase the proliferation of soil microorganisms that play an important role in determining soil fertility (Lošák et al., 2018). Statistical analysis of nitrogen content differences in Table 3. Based on the statistical analysis of differences in nitrogen, phosphorus and potassium between plants without hydrogels, it is quite different significantly from the whole plant given the addition of hydrogels, especially in the composition KTiKPAG60 which tends to have a higher content of nitrogen, phosphorus, and potassium in the soil if compared with the other composition of hydrogels. Decreased levels are precisely seen in the composition KTiKPAG80.

### 3.2.6. Statistical Analysis of Soybean Plant Growth

The results of the analysis of soybean growth statistics include plant height, number of leaves, and total dry weight can be seen in Table 4. Based on the table, it shows that the growth performance of plants without hydrogels is quite significantly different from the whole plant given the addition of hydrogels. The plants with the addition KTiKPAG60 hydrogels showed a maximum increase in growth in leaf number, plant height, and total dry weight of soybean plants.

## 4. Conclusions

Synthesis of chitosan-co-polyacrylamide-TiO<sub>2</sub> crosslinked glutaraldehyde hydrogel was carried out by chemical crosslinking method. Characterization of hydrogels using the Fourier Transform Infrared and Scanning Electron Microscope indicated that hydrogel has been successfully synthesized. The SEM

image shows the formation of pores and cavities in the hydrogel. The application of hydrogels in soybean plants shows differences in physical properties, soil chemistry, and plant growth. The use of all variations of hydrogel had no significant effect on soil physical properties including temperature, humidity, pH, and bulk density. Meanwhile, hydrogels with TiO<sub>2</sub> concentration of 60 ppm influence the soil chemical properties significantly such as organic carbon, cation exchange capacity (CEC), and level of absorbed nitrogen, phosphorus, and potassium fertilizer. The optimum number of leaves, plant height, and total dry weight are indicated by KTiKPAG60 hydrogel. The results showed that chitosan-co-polyacrylamide-TiO<sub>2</sub> crosslinked glutaraldehyde has the potential to be a soil conditioner.

## Acknowledgements

Thanks to the Directorate of Research and Community Service, Ministry of Research and Higher Education, Director of Higher Education that has funded this research, with the grants number 058/SP2H/LT/DRPM/2019. The all authors give the full thanks to Dr. L. M. Harjoni Kilowasid as the Head of Soil Laboratory, Faculty of Agriculture, Universitas Halu Oleo.

## References

- Abdel-Aziz, H.M.M., Hasaneen, M.N.A., Omer, A.M., 2016. Nano chitosan-NPK fertilizer enhances the growth and productivity of wheat plants grown in sandy soil. *Spanish Journal of Agricultural Research* 14(1), 902. <https://doi.org/10.5424/sjar/2016141-8205>
- Al-Karawi, A.J.M., Al-Qaisi, Z.H.J., Abdullah, H.I., Al-Mokaram, A.M.A., Al-Heetimi, D.T.A., 2011. Synthesis, characterization of acrylamide grafted chitosan and its use in removal of copper (II) ions from water. *Carbohydrate Polymers* 83(2), 495–500. <https://doi.org/10.1016/j.carbpol.2010.08.017>
- Bian, X., Zeng, L., Deng, Y., Li, X., 2018. The Role of Superabsorbent Polymer on Strength and Microstructure Development in Cemented Dredged Clay with High Water Content. *Polymers* 10(10), 1069. <https://doi.org/10.3390/polym10101069>
- Ciolacu, D., Oprea, A.M., Anghel, N., Cazacu, G., Cazacu, M., 2012. New cellulose-lignin hydrogels and their application in controlled release of polyphenols. *Materials Science and Engineering* 32(3), 452–463. <https://doi.org/10.1016/j.msec.2011.11.018>

**Table 4**  
Statistical analysis of growth plants

Treatment	Plant Height (cm)	Number of Leaves	Total dry Weight (g)
Kontrol	135.0a	42.3a	9.1a
KKPAG	141.0a	51.3b	14.6b
KTiKPAG10	161.3ab	54.0bc	14.5b
KTiKPAG20	176.6ab	55.7bc	15.7bc
KTiKPAG30	177.0ab	56.0bc	18.3cd
KTiKPAG40	195.3ab	60.7c	19.6d
KTiKPAG60	207.0b	68.3d	20.6d
KTiKPAG80	181.3 ab	58.3bc	19.2cd

The mean values followed by unequal letters in the same column differed significantly at 0.05 which was tested by the Duncan method.

- Dutta, J., Tripathi, S., Dutta, P.K., 2012. Progress in antimicrobial activities of chitin, chitosan and its oligosaccharides: a systematic study needs for food applications. *Food Science and Technology International* 18(1), 3–34. <https://doi.org/10.1177/1082013211399195>
- El Kadib, A., Bousmina, M., 2012. Chitosan bio based organic-inorganic hybrid aerogel microspheres. *Chemistry-A European Journal* 18(27), 8264–8277. <https://doi.org/10.1002/chem.201104006>
- Elliott, M., 2004. Superabsorbent polymers. *Prod. Dev. scientist SAP. BASF Aktiengesellschaft* ss 13.
- Gao, J., Wang, A., Li, Y., Fu, Y., Wu, J., Wang, Y., Wang, Y., 2008. Synthesis and characterization of superabsorbent composite by using glow discharge electrolysis plasma. *Reactive and Functional Polymers* 68(9), 1377–1383. <https://doi.org/10.1016/j.reactfuncpolym.2008.06.018>
- Giorgetti, L., Spanň, C., Muccifora, S., Bellani, L., Tassi, E., Bottega, S., Di Gregorio, S., Siracusa, G., di Toppi, L.S., Castiglione, M.R., 2019. An integrated approach to highlight biological responses of *Pisum sativum* root to nano-TiO<sub>2</sub> exposure in a biosolid-amended agricultural soil. *Science of The Total Environment* 650, 2705–2716. <https://doi.org/10.1016/j.scitotenv.2018.10.032>
- Gomes, L.P., Paschoalin, V.M.F., Del Aguila, E.M., 2017. Chitosan nanoparticles: Production, physicochemical characteristics and nutraceutical applications. *Revista Virtual de Quimica* 9(1), 387–409. <https://doi.org/10.3390/moleculas24010127>
- Griffin, E.A., Allen, D.G., Verboom, W.H., 2003. Paired Site Sampling for Soil Carbon Estimation-Western Australia. Australian Greenhouse Office.
- Haider, A.J., Jameel, Z.N., Taha, S.Y., 2015. Synthesis and characterization of TiO<sub>2</sub> nanoparticles via sol-gel method by pulse laser ablation. *Engineering and Technology Journal* 33, 761–771.
- Khater, M.S., 2015. Effect of titanium nanoparticles (TiO<sub>2</sub>) on growth, yield and chemical constituents of coriander plants. *Arab Journal of Nuclear Sciences and Applications* 48(4), 187–194.
- Lošák T., Ševčík M., Plchová R., von Bennewitz E., Hlušek J., Elbl J., Buňka F., Poláček Z., Antonkiewicz J., Varga L., Vollmann J. 2018. Nitrogen and sulphur fertilisation affecting soybean seed spermidine content. *Journal of Elementology* 23, 2, 581–588. <https://doi.org/10.5601/jelem.2017.22.3.1516>
- Maitra, J., Shukla, V.K., 2014. Cross-linking in hydrogels-a review. *American Journal of Polymer Science* 4(2), 25–31. <https://doi.org/10.5923/j.ajps.20140402.01>
- Maulidiyah, Azis, T., Nurwahidah, A.T., Wibowo, D., Nurdin, M., 2017. Photoelectrocatalyst of Fe co-doped N-TiO<sub>2</sub>/Ti nanotubes: Pesticide degradation of thiamethoxam under UV-visible lights. *Environmental Nanotechnology, Monitoring and Management* 8. <https://doi.org/10.1016/j.enmm.2017.06.002>
- Motsara, M.R., Roy, R.N., 2008. Guide to laboratory establishment for plant nutrient analysis. Food and Agriculture Organization of the United Nations Rome.
- Munyiri, S.W., Pathak, R.S., Tabu, I.M., Gemenet, D.C., 2010. Effects of moisture stress at flowering on phenotypic characters of selected local maize landraces in Kenya. *Journal of Animal and Plant Sciences* 8(1), 892–899.
- Nayl, A.A., Awwad, N.S., Aly, H.F., 2009. Kinetics of acid leaching of ilmenite decomposed by KOH: Part 2. Leaching by H<sub>2</sub>SO<sub>4</sub> and C<sub>2</sub>H<sub>2</sub>O<sub>4</sub>. *Journal of Hazardous Materials* 168, 793–799.
- Nurdin, M., Azis, T., Maulidiyah, M., Aladin, A., Hafid, N.A., Salim, L.O.A., Wibowo, D., 2018a. Photocurrent Responses of Metanil Yellow and Remazol Red B Organic Dyes by Using TiO<sub>2</sub>/Ti Electrode, in: *IOP Conference Series: Materials Science and Engineering*. IOP Publishing 367(1), 12048. <https://doi.org/10.1088/1757-899X/367/1/012048>
- Nurdin, M., Maulidiyah, M., Salim, L.O.A., Muzakkar, M.Z., Umar, A.A., 2018b. High performance cypermethrin pesticide detection using anatase TiO<sub>2</sub>-carbon paste nanocomposites electrode. *Microchemical Journal* 145, 756–761. <https://doi.org/10.1016/j.MICROC.2018.11.050>
- Nurdin, M., Muzakkar, M.Z., Maulidiyah, M., Maulidiyah, N., Wibowo, D., 2016. Plasmonic Silver—N/TiO<sub>2</sub> Effect on Photoelectrocatalytic Oxidation Reaction. *Journal of Materials and Environmental Science* 7(9), 3334–3343.
- Park, S.Y., Marsh, K.S., Rhim, J.W., 2002. Characteristics of different molecular weight chitosan films affected by the type of organic solvents. *Journal of Food Science* 67, 194–197(1). <https://doi.org/10.1111/j.1365-2621.2002.tb11382.x>
- Pathania, D., Gupta, D., Kothiyal, N.C., Eldesoky, G.E., Naushad, M., 2016. Preparation of a novel chitosan-g-poly (acrylamide)/Zn nanocomposite hydrogel and its applications for controlled drug delivery of ofloxacin. *International Journal of Biological Macromolecules* 84, 340–348. <https://doi.org/10.1016/j.ijbiomac.2015.12.041>
- Pivato, A., Vanin, S., Raga, R., Lavagnolo, M.C., Barausse, A., Rieple, A., Laurent, A., Cossu, R., 2016. Use of digestate from a decentralized on-farm biogas plant as fertilizer in soils: an ecotoxicological study for future indicators in risk and life cycle assessment. *Waste Management* 49, 378–389. <https://doi.org/10.1016/j.wasman.2015.12.009>
- Rafique, R., Zahra, Z., Virk, N., Shahid, M., Pinelli, E., Park, T.J., Kallerhoff, J., Arshad, M., 2018. Dose-dependent physiological responses of *Triticum aestivum* L. to soil applied TiO<sub>2</sub> nanoparticles: Alterations in chlorophyll content, H<sub>2</sub>O<sub>2</sub> production, and genotoxicity. *Agriculture, Ecosystems & Environment* 255, 95–101.
- Rajakumar, R., Sankar, J., 2016. Hydrogel: novel soil conditioner and safer delivery vehicle for fertilizers and agrochemicals—a review. *International journal of applied and pure science and agriculture* 2, 163–172.
- Rashidi, M., Seilsepour, M., 2008. Modeling of soil cation exchange capacity based on some soil physical and chemical properties. *ARPN: Journal of Agricultural and Biological Science* 3, 6–13.
- Ritonga, H., Nurfadillah, A., Rembon, F.S., Ramadhan, L., Nurdin, M., 2019. Preparation of Chitosan-EDTA hydrogel as soil conditioner for soybean plant (*Glycine max*). *Groundwater for Sustainable Development* 100277. <https://doi.org/10.1016/j.gsd.2019.100277>
- Rusan, M.J.M., Hinnawi, S., Rousan, L., 2007. Long term effect of wastewater irrigation of forage crops on soil and plant quality parameters. *Desalination* 215(1–3), 143–152.
- Rusdi, M., Roosli, R., Ahamad, M.S.S., 2015. Land evaluation suitability for settlement based on soil permeability, topography and geology ten years after tsunami in Banda Aceh, Indonesia. *The Egyptian Journal of Remote Sensing and Space Science* 18(2), 207–215.
- Sewvandi, G.A., Adikary, S.U., 2012. Synthesizing and characterization of natural biopolymer chitosan derived from shrimp type, *Penaeus monodon*. *Tropical Agricultural Research* 23(3).
- Synowiecki, J., Al-Khateeb, N.A., 2003. Production, properties, and some new applications of chitin and its derivatives. <https://doi.org/10.1080/10408690390826473>
- Weldemariam, Y., Welderfael, T., 2015. Photocatalytic degradation of methyl orange by Ag-N Co-doped ZnO nanoparticles. *Chemistry and Materials Research* 7(8), 40–49.
- Wood, A.J., Roper, J., 2000. A simple & nondestructive technique for measuring plant growth & development. *The American Biology Teacher* 62(3), 215–218.
- Yu, S., Zhang, X., Tan, G., Tian, L., Liu, D., Liu, Y., Yang, X., Pan, W., 2017. A novel pH-induced thermosensitive hydrogel composed of carboxymethyl chitosan and poloxamer cross-linked by glutaraldehyde for ophthalmic drug delivery. *Carbohydrate Polymers*. 155, 208–217. <https://doi.org/10.1016/j.carbpol.2016.08.073>
- Zhao, F., Yao, D., Guo, R., Deng, L., Dong, A., Zhang, J., 2015. Composites of polymer hydrogels and nanoparticulate systems for biomedical and pharmaceutical applications. *Nanomaterials* 5(4), 2054–2130. <https://doi.org/10.3390/nano5042054>
- Zhou, W., Yao, K., Kurth, M.J., 1996. Synthesis and swelling properties of the copolymer of acrylamide with anionic monomers. *Journal of Applied Polymer Science* 62(6), 911–915. [https://doi.org/10.1002/\(SICI\)1097-4628\(19961107\)62:6<911::AID-APP7>3.0.CO;2-S](https://doi.org/10.1002/(SICI)1097-4628(19961107)62:6<911::AID-APP7>3.0.CO;2-S)